



ELSEVIER

Soil Dynamics and Earthquake Engineering 24 (2004) 473–485

SOIL DYNAMICS
AND
EARTHQUAKE
ENGINEERING

www.elsevier.com/locate/soildyn

Three-dimensional finite element analysis of the seismic behavior of inclined micropiles

Marwan Sadek*, Shahrour Isam

Laboratoire de Mécanique de Lille (CNRS UMR 8107), Université des Sciences et Technologies de Lille (USTL), Pôlytech-Lille, 59 655 Villeneuve d'Ascq Cedex, France

Accepted 20 February 2004

Abstract

This paper presents a thorough study of the behavior of inclined micropiles under seismic loading. Analysis is carried out using a full three-dimensional finite element modeling. The soil media is assumed to be elastic with Rayleigh damping, while micropiles are modeled as 3D elastic beam elements. The structure is described by a single degree of freedom system composed of a concentrated mass and a column. The paper is composed of four parts. The first part includes a literature survey on the behavior of inclined micropiles. The second part presents the numerical model used in this study. The third part concerns analysis related to the influence of micropiles inclination on the seismic behavior of a group of micropiles embedded in a homogeneous soil with a uniform stiffness. The last part deals with the seismic behavior of inclined micropiles embedded in a soil layer with a depth-based increasing stiffness. The results of this study provide valuable information about the influence of micropiles inclination on dynamic amplification and on the seismic-induced internal forces in micropiles.

© 2004 Elsevier Ltd. All rights reserved.

Keywords: Finite element; Group; Inclination; Micropiles; Seismic; Three-dimensional

1. Introduction

The use of micropiles in seismic retrofitting or in new construction in seismic zones requires a thorough analysis of the seismic-induced response for groups of micropiles with inclined elements. As a matter of fact, as the stiffness and resistance of vertical micropiles to lateral loading is generally small, the use of inclined micropiles presents a potential alternative to withstand inertial forces and to ensure stability of the foundations system under seismic loading.

Use of micropiles in seismic area suffers from code restrictions issued on piles. The seismic role of inclined piles has been considered detrimental based on several research-based arguments such as: (i) inclined piles may induce large forces to the pile cap, or (ii) if inclination is not symmetric, permanent rotation may develop due to the varying stiffness of the pile group in each direction. According to the French recommendation (AFPS [1]),

the use of inclined piles in seismic zone is prohibited whereas soil reinforcement could contain inclined elements. The seismic Eurocode EC8 indicates that inclined piles should not be used for transmitting lateral loads to the soil, but in any case, if such piles are used they must be designed to safely carry axial as well as bending loading (Eurocode EC 8 [2]).

As reported by Gazetas and Mylonakis [3], in recent years evidence has been accumulating that inclined piles may, in certain case, be beneficial rather than detrimental both for the structure they support and the piles themselves. One supporting evidence to this issue was noted during the Kobe earthquake. It was noted that one of the few quay-walls that survived the disaster in Kobe harbor was a composite wall relying on inclined piles, conversely, the near wall, supported on vertical piles, was completely devastated. Furthermore, centrifuge tests and pseudo-static analysis carried out by Juran et al. [4] showed that pile inclination contributes to: (i) a decrease in both the pile cap displacement and bending moment at the pile-cap connections and (ii) an increase in the axial force.

This paper attempts to analyze the influence of micropiles inclination on their response to seismic loading.

* Corresponding author. Tel.: +33-3-20-43-46-30; fax: +33-3-28-76-73-01.

E-mail addresses: marwan.sadek@polytech-lille.fr (M. Sadek), isam.shahrour@polytech-lille.fr (S. Isam).

Nomenclature

$$a_0 = \omega D_p / V_s$$

dimensionless frequency

a_{cap} acceleration at the cap level

a_g amplitude of the seismic loading

a_{st} acceleration at the superstructure mass level

f_1 natural frequency of the soil layer

f_{load} frequency of the seismic loading

f_{st} natural frequency of the superstructure

m_{st} mass of the superstructure

A_p micropile section

D_p micropile diameter

Epl_p bending stiffness of micropiles

E_s Young's modulus of soil

H_{cap} horizontal loading applied at the cap

H_s thickness of the soil layer

H_{st} height of the superstructure

L_p micropile length

N axial force

N_{head} axial force at the head of micropiles

M bending moment

H_{cap} overturning moment applied at the cap

M_{head} bending moment at the head of micropiles

S micropiles spacing

T shearing force

T_{head} shearing force at the head of micropiles

V_s shear wave velocity

α micropiles inclination with regard to the vertical axis

ν_s Poisson ratio of the soil

ω pulsation

ξ_p damping ratio of the micropile

ξ_s damping ratio of the soil

Analysis is conducted using a full three-dimensional finite element analysis (FEM) with PECPLAS finite element program [5,6]. The results obtained in this study provide interesting information about the influence of micropiles inclination on seismic response of the soil–micropile–structure system. The first part of the paper presents the numerical model used in this study. The second part presents analysis of the seismic behavior of micropiles embedded in a homogeneous soil with a uniform stiffness, while the last part presents similar analysis for micropiles embedded in a soil with a depth-based increasing stiffness.

2. Numerical model

Numerical simulations were carried out using the finite element program PECPLAS [5,6]. A global three-dimensional approach is used for analysis of the micropiles–soil–structure interaction. The superstructure is modeled as a single degree of freedom system composed of a concentrated mass and a column, while 3D beam elements are used to model micropiles. The behavior of the soil and structure materials is assumed to be elastic with Rayleigh damping. The damping matrix $[C]$ results from a combination of the mass and stiffness matrices

$$[C] = a_M[M] + a_K[K] \quad (1)$$

where a_M and a_K depend on the material damping. For the i th mode, the damping ratio ξ_i is related to the natural frequency ω_i by the following relation:

$$\xi_i = \frac{a_M}{2\omega_i} + \frac{a_K\omega_i}{2} \quad (2)$$

The seismic loading is applied at the base of the soil mass as a harmonic acceleration. Lateral boundaries are placed at

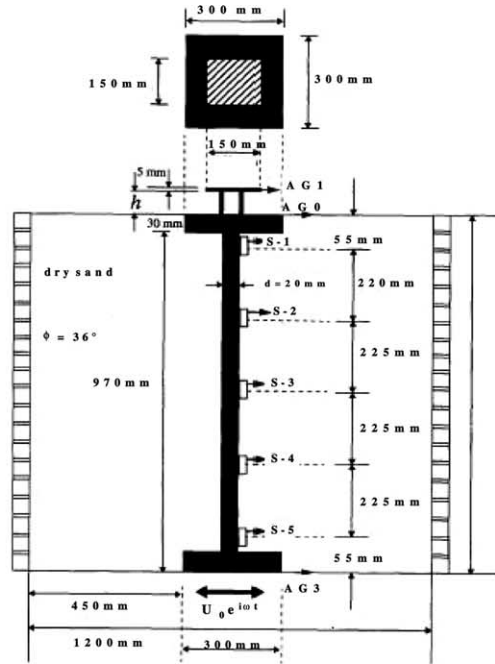
a large distance from the micropiles in order to minimize boundary effect as discussed in Ref. [6]. Periodic displacement conditions are imposed at lateral boundaries of the soil mass. Analysis is performed in the time domain using the implicit Newmark time integration scheme.

This numerical model used in this study was checked on a pile test conducted in a shaking table at Saitama University [7]. The pile supports a superstructure with a natural frequency $f_{\text{st}} = 7$ Hz. Fig. 1 shows the experimental model and summarizes its geometrical and mechanical properties. The soil behavior is assumed to be elastic with Rayleigh damping. Analysis was performed with two values of the damping factor $\xi = 10$ and 12%. The damping Rayleigh parameters a_K and a_M were determined from Eq. (2) for the loading frequency ($\omega = \omega_{\text{load}}$) assuming an equivalent contribution of the stiffness and mass matrices for damping. Fig. 1b presents a comparison of recorded and computed accelerations of the pile at depth $z = 0.275$ for different values of the dimensionless frequency $a_0 = \omega D_p / V_s$ (ω , D_p and V_s denote the loading frequency, the pile diameter and the velocity of the shear wave, respectively). Fig. 1c compares measured and computed amplitudes of strains along the pile for the dimensionless frequency $a_0 = 0.03$. It can be observed that the finite element program reproduces correctly the pile test.

3. Micropiles in a homogeneous soil (case 1)

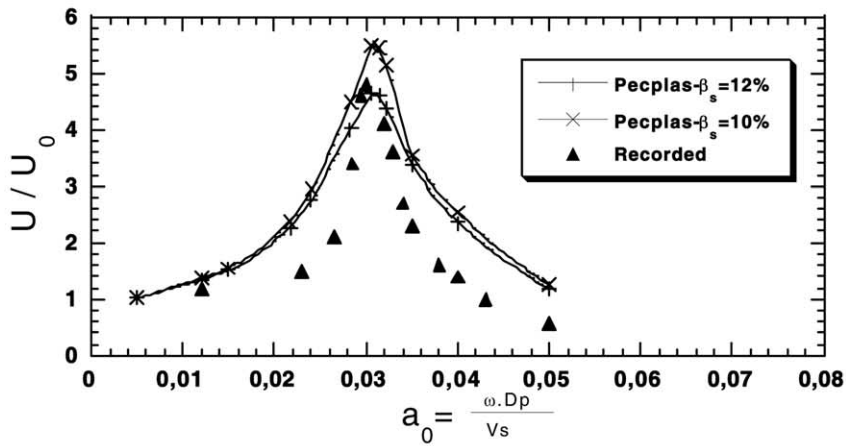
3.1. Presentation

Analysis is first performed on a group of four micropiles embedded in a homogeneous soil underlined by rigid bedrock (Fig. 2). The thickness of the soil layer is equal to $H_s = 15$ m. An elastic constitutive relation with Rayleigh damping is assumed for the soil–micropiles–structure

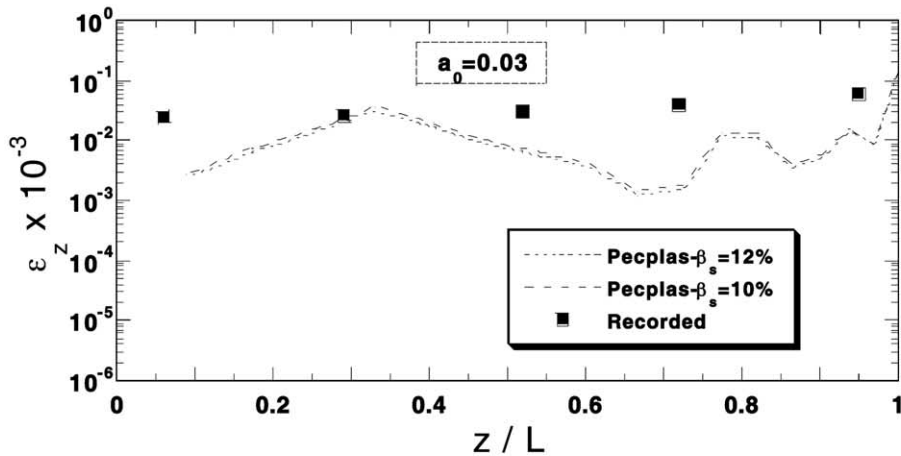


a) Experimental Model

Soil : $V_s=80$ m/s ; $\nu_s=0.4$.
 Structure: Mass = 0.885 kg; $H_s=107$ mm.
 Pile: $D_p = 0.02$ m, thickness 1.0 mm.
 Cap: Mass = 21.27 kg.



b) Acceleration transfer functions at depth $z=0.25$ m



c) Strain amplitude along the pile

Fig. 1. Verification of the numerical model on a pile test conducted using a shaking table (After Makris et al. [7]).

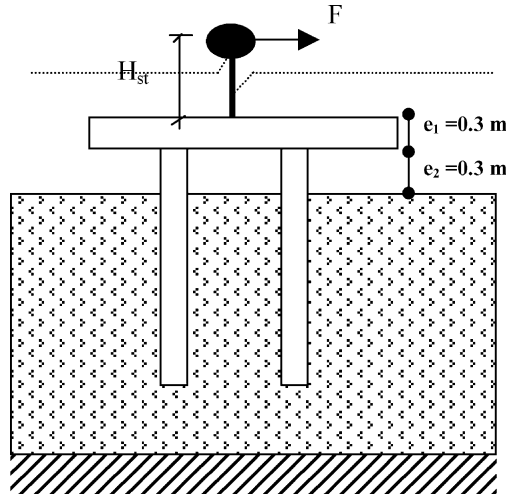


Fig. 2. Problem under consideration.

system. Analysis was carried out with the following characteristics for the soil material: Young's modulus of the soil $E_s = 8$ MPa, Poisson's Ratio $\nu_s = 0.45$, damping factor $\xi_s = 5\%$. The fundamental frequency of the soil layer is equal to $f_1 = 0.67$ Hz ($4V_s/H_s$, where V_s is the shear wave velocity, H_s is the thickness of the soil layer).

Micropiles spacing ratio is equal to $S/D_p = 5$, D_p denotes the micropile diameter. The micropile length is $L_p = 10$ m, its axial and flexural rigidities are, respectively, $E_p A_p = 1100$ MN and $E_p I_p = 0.85$ MN m². The structure is modeled as a single degree of freedom system composed of a concentrated mass $m_{st} = 40$ ton, and a column with a height $H_{st} = 1$ m. Its fixed base fundamental frequency is equal to $f_{st} = 1.36$ Hz. Micropiles are connected to a cap which is free of contact with the soil. The thickness of the cap is equal to 0.3 m. The mechanical properties of the soil and micropiles are summarized in Table 1.

The finite element mesh used in the numerical simulations for inclined micropiles is shown in Fig. 3. It includes 21,576 8-node elements and 34 3D-beam elements. Lateral

Table 1a
Properties of the soil material

Case	Mass density (kg/m ³)	Young's modulus	Poisson's ratio	Damping ratio
Case 1: constant stiffness	$\rho_s = 1700$	8 MPa	$\nu_s = 0.45$	$\xi_s = 5\%$
Case 2: depth-increasing stiffness	$\rho_s = 1700$	$E_s(z) = E_{s0} \left(\frac{p(z)}{p_a} \right)^{0.5}$	$\nu_s = 0.45$	$\xi_s = 5\%$
		$p(z) = \frac{(1 + 2K_0)\gamma z}{3}$		
		if $z < z_0$, $p(z) = p(z_0)$		
		$E_{0s} = 10$ MPa;		
		$p_a = 100$ kPa		

Table 1b
Properties of micropiles

Bending stiffness (MN m ²)	Axial stiffness (MN)	Damping ratio	Length (m)
$E_p I_p = 0.85$	$E_p A_p = 1100$	$\xi_p = 2\%$	$L_p = 10$

boundaries are placed at a distance $R_1 = 60$ m ($240 D_p$) from the central axis of the micropile-group in order to minimize any boundary effect as discussed in Ref. [6].

The seismic loading is applied at the base of the soil mass as a harmonic acceleration. The amplitude of the load is $a_g = 0.2$ g, while its frequency (f_{load}) is assumed to be equal to the fundamental frequency of the soil layer ($f_1 = 0.67$ Hz).

3.2. Group of vertical micropiles

Fig. 4 depicts the maximum horizontal acceleration and internal forces induced in the group of vertical micropiles due to seismic loading. The amplification of the lateral acceleration at the micropiles cap a_{cap}/a_g is equal to 13.7. At the superstructure mass level, the amplification of the acceleration a_{st}/a_g attains a value of 17.88. This value is about 30% higher than (a_{cap}/a_g) ratio. This value clearly emphasizes the necessity to take into account the dynamic amplification in the structure for any pseudo-static analysis. In this case the maximum inertial force induced by the seismic loading is $F_{in} = 1430$ kN ($M_{st} a_{st}$). At the micropiles cap level, it induces a horizontal force (H_{cap}) = 1430 kN and a moment (M_{cap}) = 1430 kN m. Note that $M_{cap} = F_{in} H_{st}$, where H_{st} is the structure height.

The profiles of the maximum bending moment and shearing force clearly show the presence of a high inertial effect, which emerges in high values of internal forces in the vicinity of the micropiles head. The profile of the bending moment depicts two peaks. The first one is induced at the micropiles head ($M_{head} = 149$ kN m), while the second appears in the central part of the micropile ($M_{central} = 12$ kN m). The ratio between the maximum bending moments M_{head} and $M_{central}$ is equal to 12.5. The profile of the axial force indicates a regular decrease with depth. At the micropile head the axial force is equal to $N_{head} = 943$ kN. It is due to both the shearing force (H_{cap}) and the moment (M_{cap}) induced by the inertial force. Since M_{cap} induces at the head of each micropile an axial force ($N_{M_{cap}} = 572$ kN m ($M_{cap}/(2S)$), the shearing force (H_{cap}) causes a significant axial force which is equal to 371 kN m. This value presents about 40% of the maximum axial force at the micropile head.

Fig. 4c shows the profile of the shearing force T . It indicates high values of T in the vicinity of the cap, followed by a sharp decrease with depth. The maximum shearing force is induced at the head of the micropile

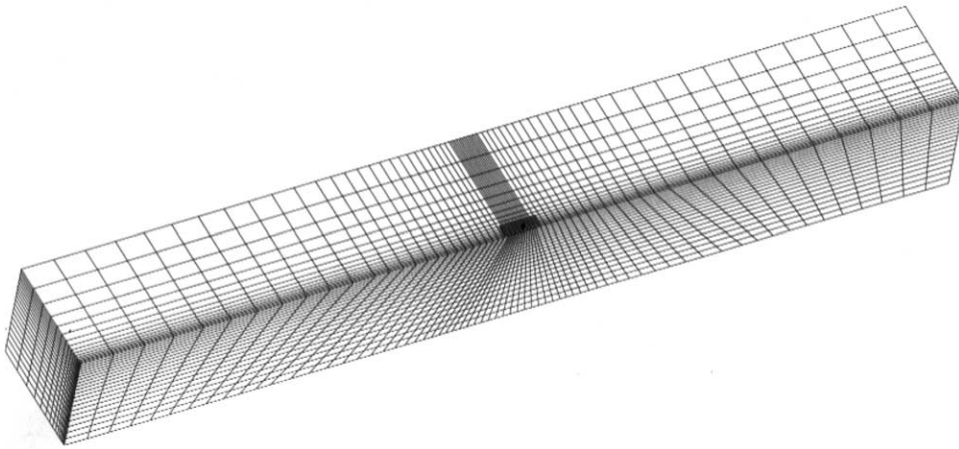


Fig. 3. 3D mesh used in the analysis of the soil–micropile–structure system (21,576 8-node elements).

($T_{\text{head}} = 355$ kN. It is equal to 25% of the inertial shearing force (H_{cap}).

The ratio of the maximum axial stress due to the axial force (N_{head}/A_p , where A_p is the area of the micropile cross-section) to that induced by the bending moment ($M_{\text{max}}D_p/(2I_p)$, I_p is the inertial moment of the micropiles section) is equal to 0.1. This ratio clearly indicates that seismic loading causes severe bending at the micropiles head, which may lead to failure at the cap-micropile connection.

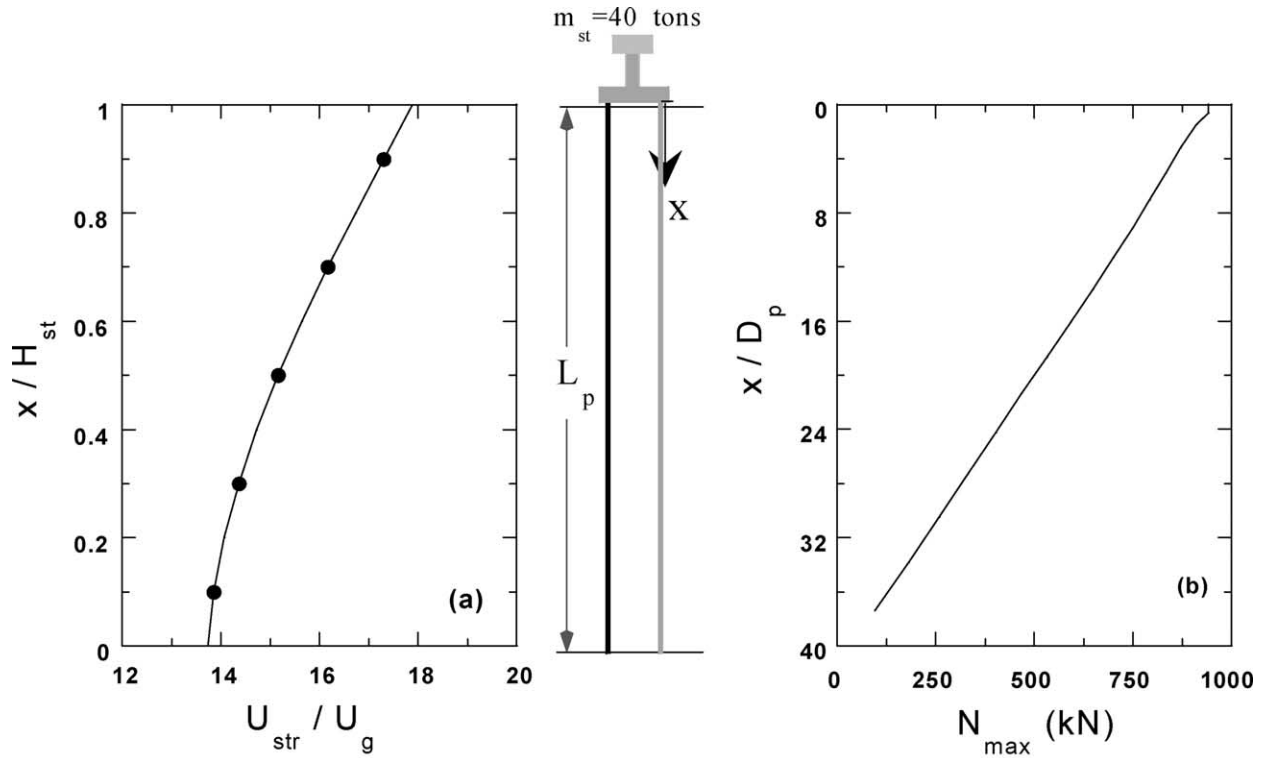
3.3. Group of inclined micropiles

Fig. 5 shows results obtained for a group of micropiles with an inclination angle (α) = 20° with respect to the vertical axis. It can be observed that seismic-induced lateral acceleration is smaller than that induced in the vertical micropile case. The amplification in the lateral acceleration at the structure mass level is (a_{st}/a_g) 13.7, which is about 20% smaller than the one induced in the structure supported by vertical micropiles.

Fig. 5b–d displays the maximum associated internal forces in the micropiles. It can be observed that the inclination of micropiles induces an important decrease in the maximum bending moment at the head of micropiles. Indeed the maximum bending moment is reduced to the half compared to that obtained with vertical micropiles. This decrease is due to both the inclination and the reduction of lateral acceleration at the top of superstructure, which induces lower moment M_{cap} at the cap level. On the other hand, inclination of micropiles induces an important reduction in the shearing force and an increase in the axial force at the micropile head. The maximum shearing force is equal to 44 kN which is about 12.5% of that induced in vertical micropiles. The maximum axial force at the micropile head is ($N_{\text{head}} = 860$ kN, which is close to that obtained with the vertical micropile. The variation of the maximum axial

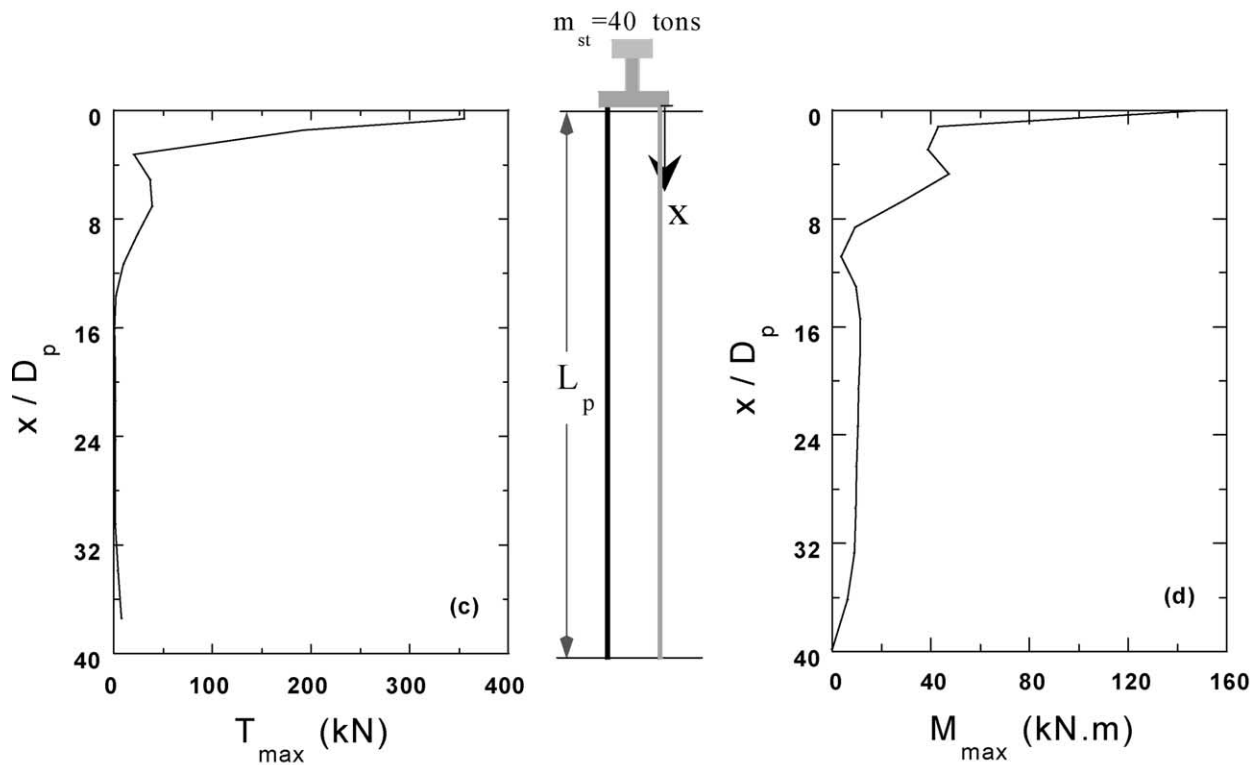
force for inclined micropiles presents trends, which are different from that observed using vertical micropiles. Indeed, the later indicates a regular decrease of N_{max} with depth, while the former shows first an increase with depth up to a peak value, that followed by a decrease. The increase in the axial force is due to the lateral displacement of the soil, which induces an axial component in the micropiles. The peak of the axial force is equal to (N_{peak}) 1590 kN, which is 69% higher than that induced at the micropile head. It is worth noting that the increase in the axial force with depth is expected to be overestimated because of the elastic constitutive relation used in this study and the hypothesis of perfect cohesion between the micropile and the soil.

The influence of micropiles inclination on their natural frequencies was investigated using the procedure proposed by Gohl [8] and Tufenkjian and Vucetic [9]. The acceleration response spectrum was determined using the Fourier analysis of the free response of the group of micropiles (Fig. 6a). Fig. 6b and c shows the spectra obtained at the mass and cap levels. It can be noted that these spectra present three peaks. The first peak for both the superstructure mass and cap accelerations is equal to the fundamental frequency of the soil layer, which means that the micropiles inclination does not affect the natural frequency of the soil–micropile–structure system. Calculations performed with inclined micropiles for the loading frequencies $f_{\text{load}} = 0.65$ and 0.68 Hz confirm this result (Table 2). They show that amplifications corresponding to these frequencies are lower than that obtained at the natural frequency of the soil layer ($f_{\text{load}} = f_1$). The second peak for the acceleration of the superstructure mass is equal to 1.28 Hz for both vertical and inclined micropiles, it corresponds to the fundamental frequency of the flexible-base-structure which is about 6% lower than that of the fixed-base-structure ($f_{\text{st}} = 1.36$ Hz). This result indicates that micropiles inclination affects slightly the natural frequency of the superstructure. Fig. 6c shows that



Amplification of the lateral acceleration in the superstructure

Maximum Axial forces in micropiles



Maximum shearing force in micropiles

Maximum bending moment in micropiles

Fig. 4. Response of a group of vertical micropiles to the seismic loading (case 1: uniform stiffness).

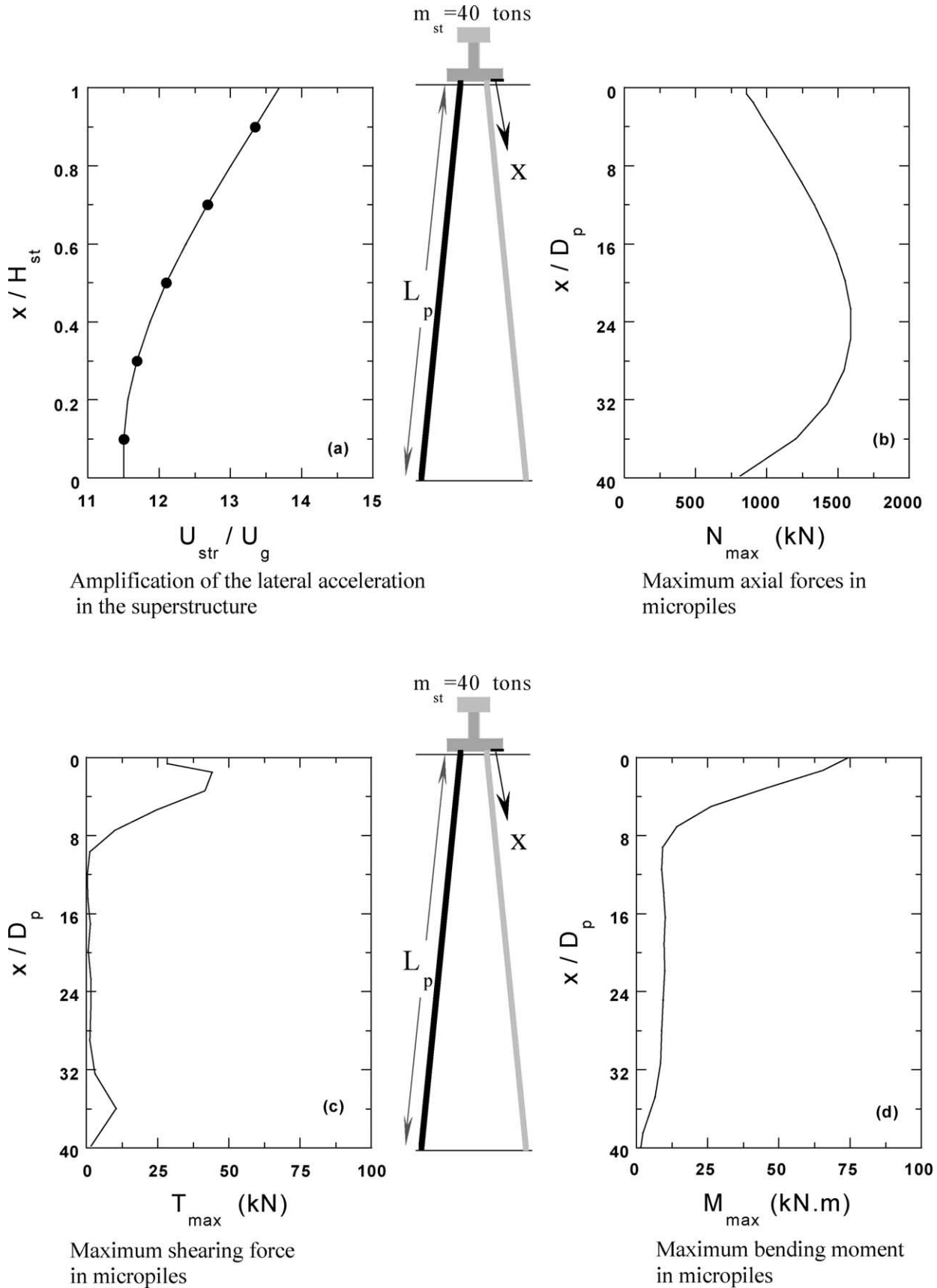
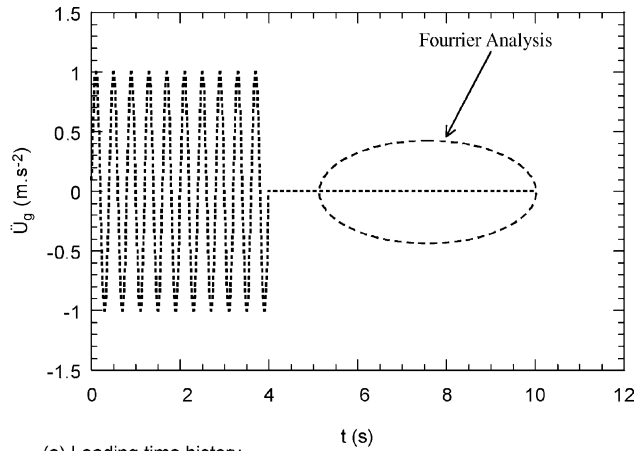
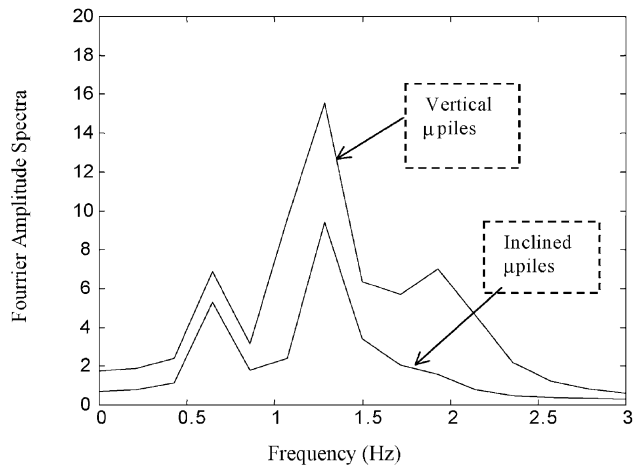


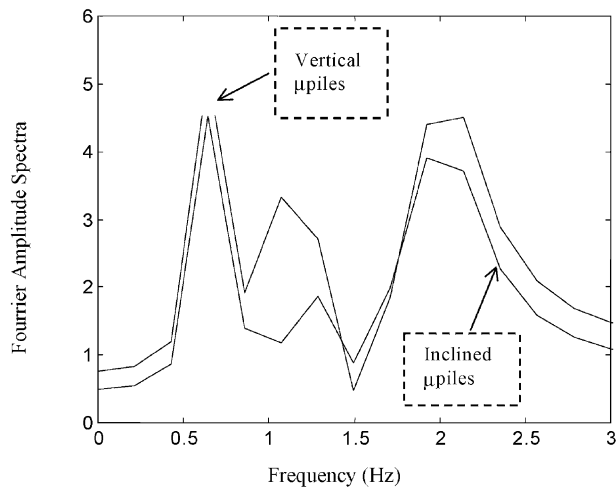
Fig. 5. Response of a group of inclined micropiles ($\alpha = 20^\circ$) (case 1).



(a) Loading time history



(b) Spectra of the acceleration at the Mass level



(c) Spectra of the acceleration at the Cap level

Fig. 6. Influence of micropiles inclination on the natural frequencies of the soil–micropile system.

the second peak of the acceleration of the affected by micropiles inclination. It increases from 1.08 to 1.28 when micropiles inclination augments from 0 to 20°. This result agrees with results of centrifuge tests reported by Juran et al.

Table 2

Dynamic amplification in the vicinity of the fundamental frequency of the soil layer

Frequency	At the structure level (a_{st}/a_g)	At the cap level (a_{cap}/a_g)
$f_{load} = 0.65$ Hz	12.1	10.2
$f_{load} = 0.68$ Hz	13.4	11.2
$f_{load} = f_1$ (0.67 Hz)	13.7	11.5

[4], which indicate that the inclination of micropiles leads to an increase in their lateral stiffness and consequently to an increase in the natural frequency of the micropile–soil system.

Fig. 7a–c and Table 3 summarize results of the numerical simulations obtained for four values of micropiles inclination namely $\alpha = 0, 7, 13$ and 20° . For convenience, internal forces will be presented in term of the following dimensionless quantities:

- Axial force: $(2N \cos(\alpha)S_p)/(m_{st}a_{st}H_{st})$.
- Shearing force: (T/N_{head}) .
- Bending moment: $(4M)/(m_{st}a_{st}H_{st})$.

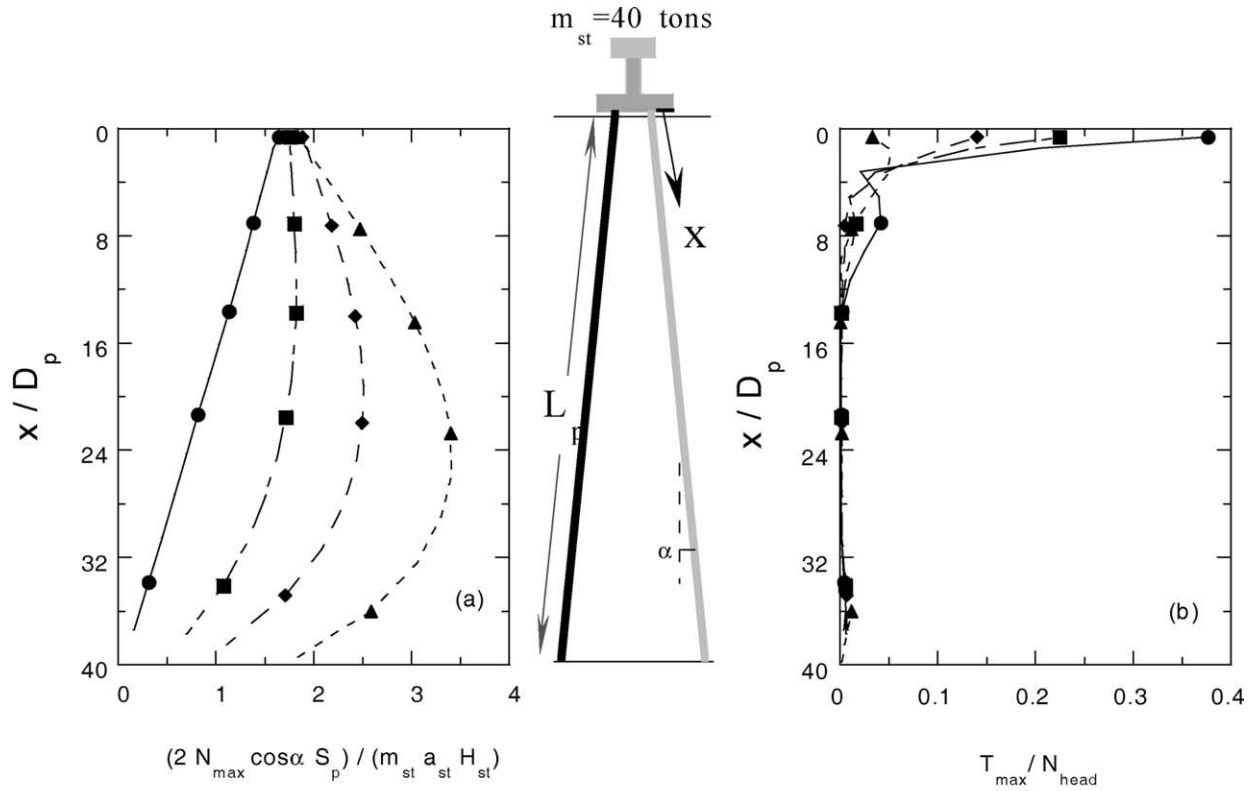
Table 3 indicates that the increase in micropile inclination from 0 to 20° induces a regular decrease in the amplification of the lateral acceleration (a/a_g), which attains 16 and 23% at the cap and the superstructure mass, respectively.

By further examination of Fig. 7a–c, it can be observed that an increase in the micropiles inclination causes a regular variation in the internal forces. In this case, inclination induces an augmentation in the axial force at the micropiles head as well as the formation of a peak for inclined micropiles in their central part. The influence of the inclination is particularly significant on the distribution of the normalized shearing force in the vicinity of micropiles head. It leads to a significant decrease with increasing the inclination of micropiles. The influence of micropiles inclination on the normalized bending moment is observed in the upper part of micropiles. The increase in α from 0 to 20° induces a decrease of about 35% in the bending moment at the micropiles head.

4. Soil with depth based-increasing stiffness (case 2)

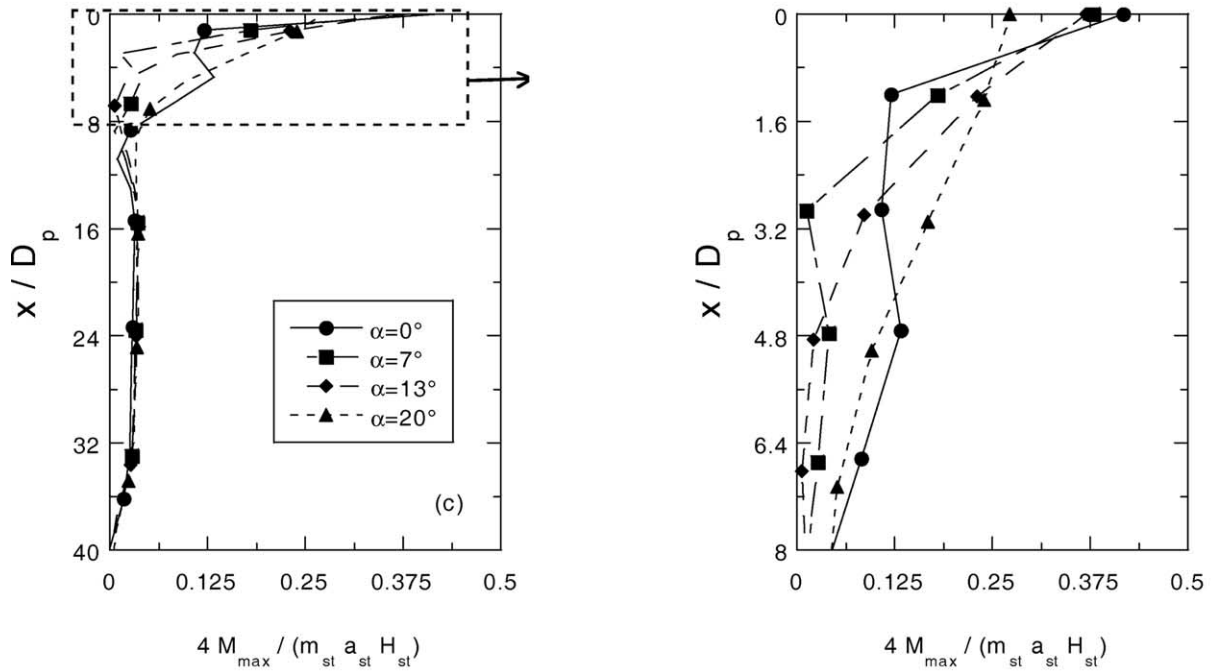
4.1. Presentation

Since soil stiffness increases with depth, this section presents FEM analysis related the behavior of inclined micropiles embedded in a soil layer having a depth based-increasing stiffness. The Young’s modulus of the soil is assumed to increase with depth according to the following



(a) Normalized axial force

(b) Normalized shearing force



(c) Normalized bending moment

(d) Zoom of Normalized bending moment

Fig. 7. Influence of inclination on the seismic response of the group of micropiles (case 1).

Table 3
Influence of the inclination on the seismic response of micropiles (case 1; $E_s = \text{constant}$)

Inclination (α)	0°	7°	13°	20°
Cap: a_{cap}/a_g	13.73	12.83	12.19	11.50
Mass: a_{st}/a_g	17.88	16.09	14.86	13.70
$\frac{2N_{\text{head}} \cos \alpha S_p}{m_{\text{st}} a_{\text{st}} H_{\text{st}}}$	1.65	1.83	1.96	1.84
$\frac{T_{\text{head}}}{N_{\text{head}}}$	0.38	0.23	0.15	0.03
$\frac{4M_{\text{head}}}{m_{\text{st}} a_{\text{st}} H_{\text{st}}}$	0.42	0.39	0.38	0.27

relation

$$E_s(z) = E_{s0} \left(\frac{p(z)}{p_a} \right)^{0.5} \tag{3}$$

where p denotes the mean stress due to the soil self-weight which is expressed as

$$p(z) = \frac{(1 + 2K_0)\gamma z}{3} \text{ if } z < z_0, \quad p(z) = p(z_0) \tag{4}$$

where z denotes depth, p_a is a reference pressure (100 kPa), E_{s0} designates the Young’s modulus for $p = p_a$; K_0 is the coefficient of lateral earth pressure at rest, z_0 designates the thickness of the soil layer that is closest to the surface, which is assumed to have a constant Young’s modulus. Numerical simulations were performed with $E_{s0} = 10 \text{ MPa}$, $K_0 = 0.5$, $z_0 = 1 \text{ m}$. The variation of the Young’s modulus with depth is shown in Fig. 8. It can be observed that the soil stiffness of the soil layer is smaller (for $z < 39D_p$) than the value assumed for the constant soil-stiffness case. The natural frequency of the soil layer was calculated according to the procedure used by Gohl [8] and Tufenkjian and Vucetic [9]. It is equal to $f_1 = 0.43 \text{ Hz}$. It is worth noting that this value is smaller than that obtained for the soil layer with uniform soil stiffness (case 1, $f_1 = 0.67 \text{ Hz}$).

The seismic loading is applied at the base of the soil mass as a harmonic acceleration whose amplitude and frequency are equal to $a_g = 0.2 \text{ g}$ and $f_{\text{load}} = 0.43 \text{ Hz}$ (f_1). The fixed base fundamental frequency of the superstructure is maintained to $f_{\text{st}} = 1.36 \text{ Hz}$.

4.2. Groups of vertical micropiles

Fig. 9 shows the influence of the soil stiffness variation in the soil layer on the overall response for the group of vertical micropiles. It can be noted that the amplification of the acceleration in the superstructure for case 2 ($a_{\text{st}}/a_{\text{cap}} = 1.14$) is smaller than that obtained in case 1 ($a_{\text{st}}/a_{\text{cap}} = 1.3$).

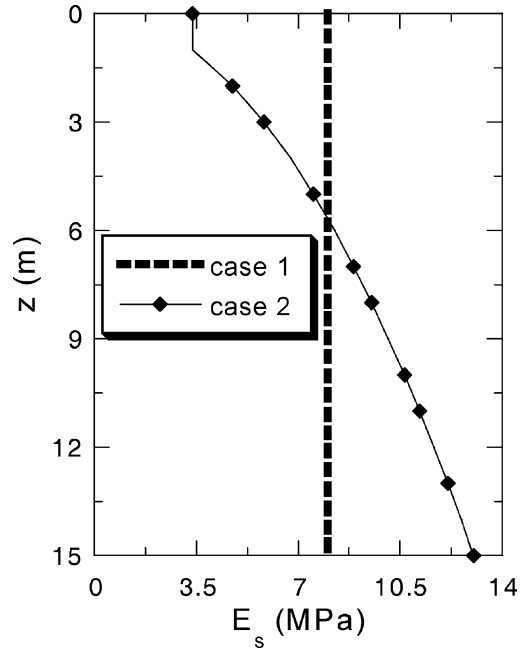


Fig. 8. Profile of the Young’s modulus for cases 1 and 2.

This result is due to the fact that the natural frequency of the soil in case 1 ($f_{\text{st}}/f_1 = 2$) is closer to the superstructure natural frequency than that in case 2 ($f_{\text{st}}/f_1 = 3.1$). This observation agrees well with those obtained by Shahrour et al. [6].

Referring to Fig. 9, it can also be observed that the distribution of the soil stiffness affects the axial force and the bending moment profiles. Indeed, the maximum bending moment in case 2 exceeds by about 172% the peak bending moment predicted for case 1. The influence of the variation in E_s on the axial force is more moderate; N_{max} in case 2 is about 14% higher than that obtained in case 1. The increase in the bending moment is due to the reduction of the soil stiffness near the soil surface, which leads to an augmentation of the lateral soil deformation and consequently causes higher bending moment in comparison with that obtained in case 1. On the other hand, it can be noted that the influence of this variation on the shearing force distribution is moderate. Its maximum values occurred at the head is governed by the acceleration at the mass level (7% variation between cases 1 and 2).

4.3. Group with inclined micropiles

Fig. 10 and Table 4 illustrate the influence of inclination on the seismic response of micropiles. Compared with the homogeneous soil case, same trends are observed. The lateral acceleration in the superstructure decreases with the increase in the micropiles inclination. The augmentation of the micropiles inclination from 0 to 20° leads to a decrease in (a_{st}/a_g) from 16.67 to 9.88 and to a decrease in (a_{cap}/a_g) from 14.61 to 10.14.

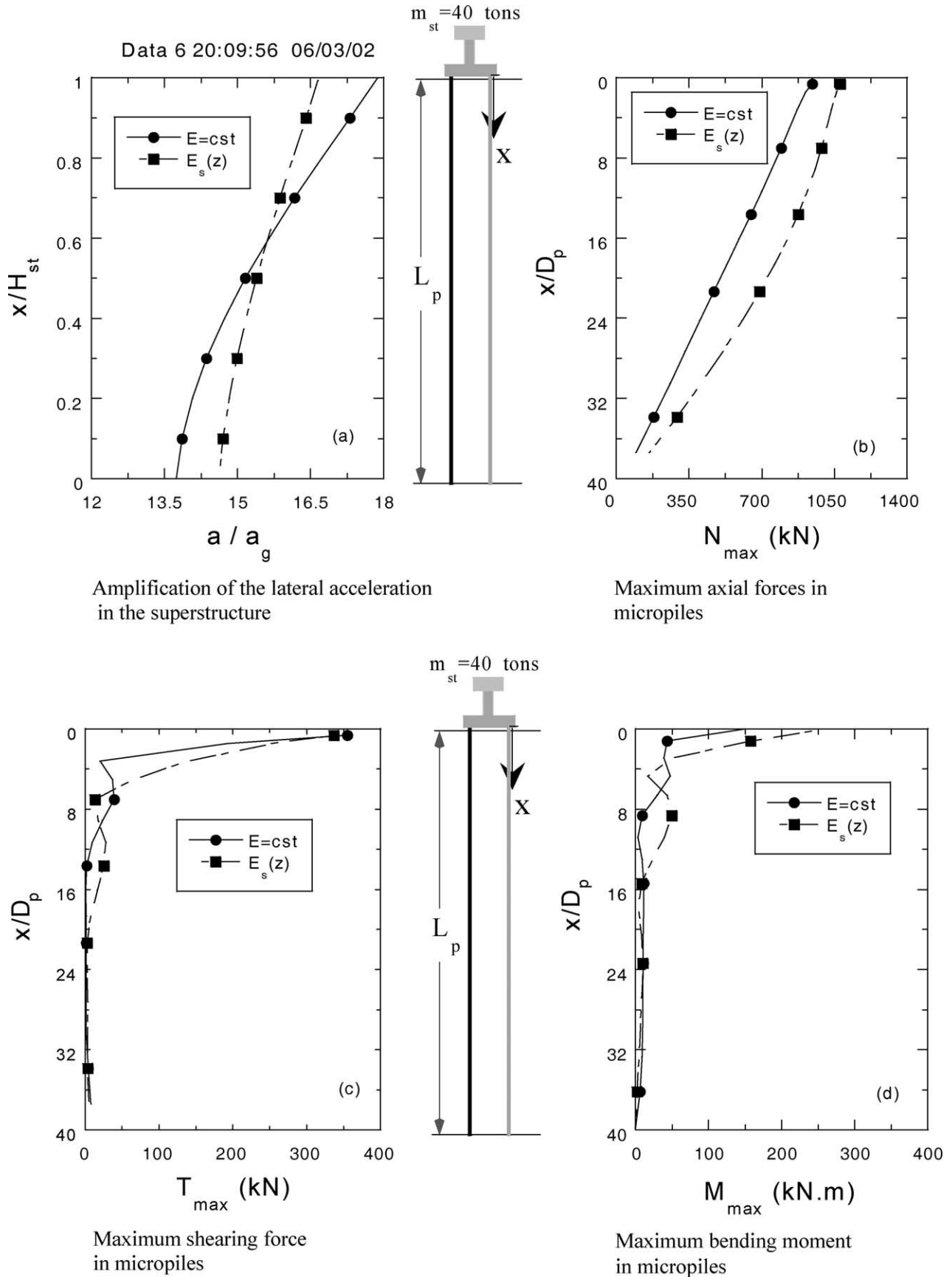


Fig. 9. Influence of the soil stiffness profile on the response of a group of vertical micropiles to the seismic loading.

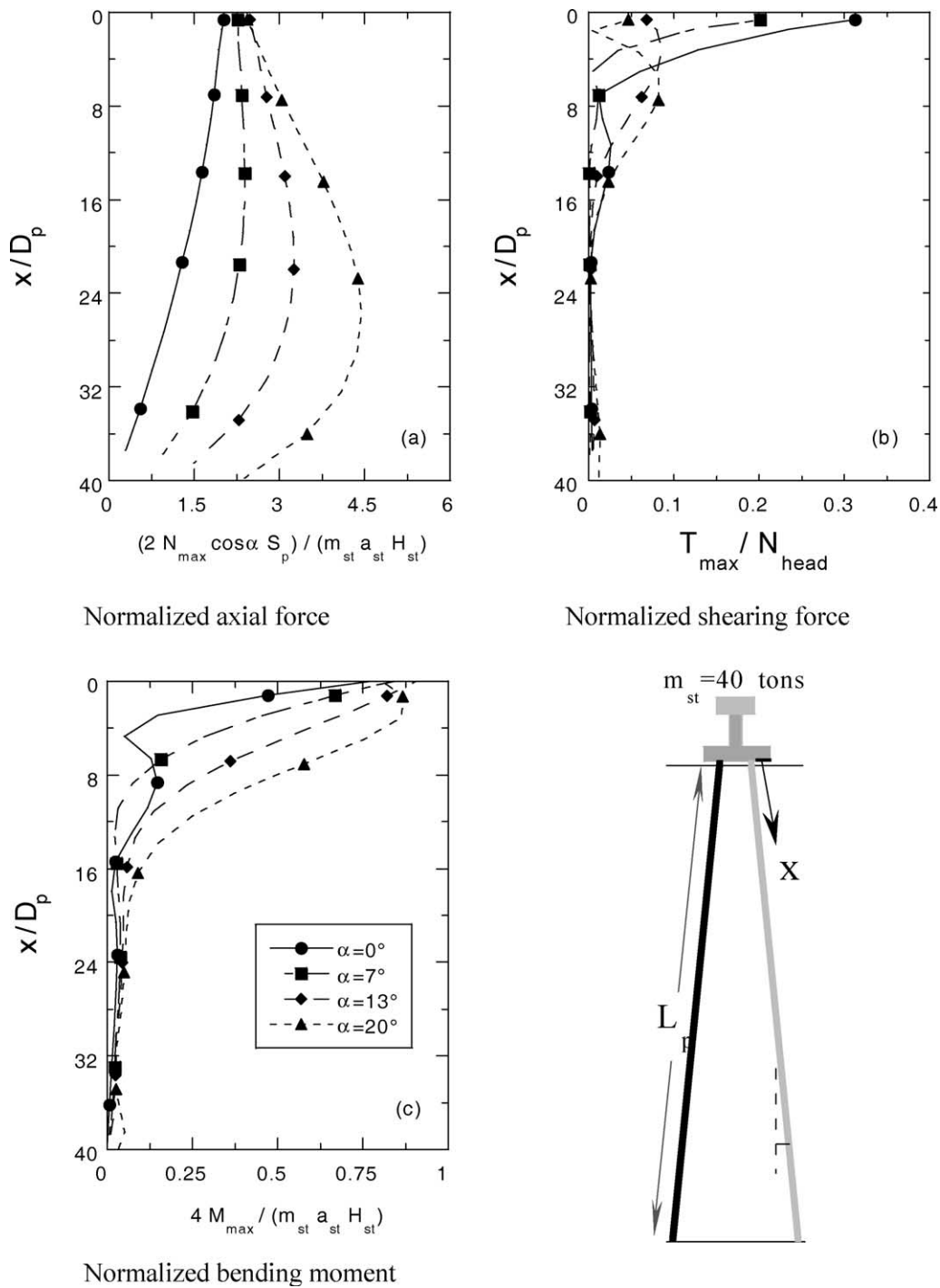


Fig. 10. Influence of inclination on the seismic response of the group of micropiles (case 2).

Fig. 10a–c clearly shows that the increase in micropiles inclination strongly affects the distribution of internal forces in micropiles. While the increase in the micropiles inclination does not strongly affect the maximum normalized bending moment M_n , it causes an increase in the normalized axial force from 2.01 to 4.44 (an increase of 220%) when the inclination increases from

0 to 20°. The normalized shearing force (Fig. 10b) shows a different trend profiles. The maximum normalized shearing at the head of micropiles decreases from 0.312 for vertical micropiles to 0.201 for $\alpha = 7^\circ$, and reaches a value of 0.08 for $\alpha = 20^\circ$. For this inclination, the maximum shearing force reaches a peak value of about 0.082 at depth $z = 7D_p$.

Table 4
Influence of the inclination on the seismic response of micropiles (case 2;
 $E_s = E_{s(z)}$)

Inclination (α)	0°	7°	13°	20°
a_{cap}/a_g	14.61	12.56	11.33	10.14
$\frac{a_s/a_g}{2N_{\text{head}} \cos \alpha S_p}$	16.67	13.42	11.55	9.88
$\frac{m_{\text{st}} a_{\text{st}} H_{\text{st}}}{2N_{\text{head}} \cos \alpha S_p}$	2.02	2.26	2.48	2.43
$\frac{T_{\text{head}}}{N_{\text{head}}}$	0.31	0.20	0.07	0.06
$\frac{4M_{\text{head}}}{m_{\text{st}} a_{\text{st}} H_{\text{st}}}$	0.77	0.84	0.90	0.80

5. Conclusion

This paper utilizes a three-dimensional finite element modeling to analyze the influence of micropiles inclination on their response to seismic loading. The study was conducted for two cases, which concern micropiles embedded in a homogeneous soil layer with a constant stiffness and a soil layer with a depth based-increasing stiffness.

Numerical simulations presented herein, show that inclination of micropile improves micropile's performance with respect to seismic loading. The inclination allows a better mobilization of the axial stiffness of micropiles and consequently leads to a decrease in both

shearing forces and bending moment induced by seismic loading.

References

- [1] AFPS. Association française de Génie Parasismique. Recommandations AFPS 90. Presses des Ponts et Chaussées; 1990.
- [2] Eurocode EC8. Structures in seismic regions. Part 5. Foundations, retaining structures, and geotechnical aspects; 1994.
- [3] Gazetas G. Mylonakis George seismic soil–structure interaction: new evidence and emerging issues. Geotechnical Earthquake Engineering and Soil Dynamics, Geo-Institute ASCE Conference, Seattle; 3–6 August, 1998.
- [4] Juran I, Benslimane A, Hanna S. Engineering analysis of dynamic behavior of micropile systems. Transportation Research Record No. 1772. Soil Mech 2001;91–106.
- [5] Sadek M, Shahrour I. Three-dimensional finite element analysis of the seismic behavior of inclined micropiles. In: Mestat P, editor. Fifth European Conference, Numerical Methods in Geotechnical Engineering. Paris: Presses de l'ENPC/LCPC; 2002. p. 995–1002.
- [6] Shahrour I, Sadek M, Ousta R. Seismic behavior of micropiles used as foundation support elements: three-dimensional finite element analysis. Transportation Research Record No. 1772. Soil Mech 2001;2001: 84–91.
- [7] Makris N, Tazoh T, Yun X, Fill AC. Prediction of the measured response of a scaled soil-pile-superstructure system. Soil Dyn Earthquake Engng 1997;16:113–24.
- [8] Gohl WB. Response of pile foundations to simulated earthquake loading. Experimental and analytical results. Thesis Submitted in Partial Fulfillment of the Requirements for the Degree of Doctor of Philosophy. The University of British Columbia; 1991.
- [9] Vucetic M, Tufenkjian M, Doroudian M. Dynamic centrifuge testing of soil nailed excavations. ASTM Geotech Test J 1993;16(2): 172–87.